EFFECT OF TOPOGRAPHIC CHARACTERISTICS ON COMPOUND TOPOGRAPHIC INDEX FOR IDENTIFICATION OF GULLY CHANNEL INITIATION LOCATIONS

H. G. Momm, R. L. Bingner, R. R. Wells, J. R. Rigby, S. M. Dabney

ABSTRACT. *Sediment loads from gully erosion contribute to water quality problems, reduction in crop productivity by removal of nutrient-rich topsoil, and damage to downstream ecosystems. The identification of areas with high potential for gully channel development is often performed using spatially derived stream power estimates from second-order topographic indices, such as the compound topographic index (CTI). The utilization of CTI to identify where gullies develop is affected by field and local topographic characteristics and DEM resolution. In this study, the effect of overall terrain slope, local relief variance, and raster grid cell size on CTI cumulative distribution values was investigated using theoretical and observed catchment methodology. In the theoretical analysis, stochastic methods were used to generate simulated catchments to quantify the influence of overall terrain slope, local relief variance, and raster grid cell size (each considered individually). The observed methodology used three sites with distinct topographic characteristics, measured gully channels, and high-resolution topographic information. Raster grids for the three observed study sites were generated at varying raster grid cell sizes. Critical CTI values were determined through comparison of measured gully thalwegs with threshold CTI raster grids of the observed watersheds at different resolutions. Results from the theoretical investigation indicate that CTI values were linearly influenced by changes in relief variance and overall slope, while variations in raster grid cell size caused an inverse power variation in CTI values. In addition, variations in raster grid cell size, produced changes in cumulative distributions of the top 0.1% CTI values. The use of normalized CTI values (CTI_n) produced merged cumulative distribution curves when varying overall slope, terrain relief variance, and to a lesser degree DEM resolution. Similar findings were obtained from the analysis of observed catchments. When DEM resolution varied, the differences in critical CTI_n values in the same field were significantly reduced when compared to original critical CTI values, although differences were not fully eliminated. Normalization of the CTI cumulative distributions improved comparisons between different sites with distinct drainage area sizes and topographic characteristics, providing a possible alternative for investigations of large watersheds with more than one topographic characteristic. Results suggest that a normalized critical CTI between 1 and 2 could be used for the identification of areas with high potential for gully development. Knowing where gullies develop is important in understanding the effect of conservation practices on soil erosion through the use of field-scale and watershed-scale simulation models. Effective watershed management plans depend on this information to target the placement of conservation practices for the efficient use of available resources.*

Keywords. *Compound topographic index, DEM resolution, Gully erosion, Random field simulation, Watershed models.*

Gully erosion can pose a serious threat to the sustainability of agriculture. Sediment loads from gully erosion sources can be a significant contributing factor to water quality problems, reduction in crop productivity by removal of nutrient-rich topsoil, and damage to downstream ecosystems (Gordon et al., 2008; Bingner et al., 2010; Poesen et al., 2003; Valentin et al., 2005). Improved evaluation techniques for areas prone to gully initiation can help target conservation measures on large watersheds, optimizing the use of farming and conservation resources (Bingner et al., 2010). Watershed models describing gully processes, such as the USDA's Annualized Agricultural Nonpoint Source (AnnAGNPS) pollution model (Bingner and Theurer, 2001), also rely on locating these source areas when

Submitted for review in February 2012 as manuscript number SW 9662; approved for publication by the Soil & Water Division of ASABE in March 2013. Presented at the 2011 Symposium on Erosion and Landscape Evolution (ISELE) as Paper No. 11050.

Mention of company or trade names is for description only and does not imply endorsement by the USDA. The USDA is an equal opportunity provider and employer.

The authors are **Henrique G. Momm,** Assistant Professor, Department of Geosciences, Middle Tennessee State University, Murfreesboro, Tennessee; **Ronald L. Bingner, ASABE Member,** Agricultural Engineer, **Robert R. Wells**, Research Hydraulic Engineer, **James R. Rigby**, Research Hydrologist; and **Seth M. Dabney, ASABE Member,** Supervisory Research Agronomist, USDA-ARS National Sedimentation Laboratory, Oxford, Mississippi. **Corresponding author:** Henrique G. Momm, Kirksey Old Main 322G, Middle Tennessee State University, Murfreesboro, TN 37132; phone: 615-904-8372; e-mail: henrique.momm@mtsu.edu.

evaluating the effect of conservation practices. Estimating areas that have a high probability of forming gully channels can be accomplished through spatial estimation of stream power from topographic information, which is widely available digitally (Wilson and Gallant, 2000). This provides an efficient and time-saving approach in developing gully characteristics at field and watershed-scales due to the difficulty of collecting the necessary parameters required for conservation management evaluation technology.

Topography has been recognized as a key factor controlling surface runoff, subsurface water movement, and the spatial distribution of zones of different moisture content and saturation, but topography is not the only factor influencing gully channel initiation (Moore et al., 1988). Once erosion begins, one of the most important factors affecting sediment transport is the potential energy of overland flow, often described in terms of potential energy dissipation per unit weight of water, or, more simply, unit stream power (Moore and Burch, 1986). Unit stream power is a function of discharge, slope, and channel width (Thorne et al., 1984). The use of drainage area as a surrogate for discharge as related to sediment transport capacity is common (Mitasova et al., 1996). Terrain slope is also often used in hydrological studies as the gradient for overland flow velocity (Moore et al., 1991). Consequently, drainage area multiplied by slope provides a proxy parameter for local stream power. This approach justifies the inclusion of both slope and drainage area in methods to estimate locations susceptible to channel initiation (Moore et al., 1988; Montgomery and Dietrich, 1992). The terrain curvature perpendicular to aspect (direction of highest change in slope) is referred to as planform curvature (Zevenbergen and Thorne, 1987) and represents the degree of convergence (concave) or divergence (convex) of the terrain. A converging profile concentrates flow, accelerates flow velocity, and implies a high rate of potential energy dissipation (Moore and Burch, 1986; Mitasova et al., 1996). Thorne et al. (1986) developed a methodology by which proxy stream power estimates (compound topographic index, CTI) are derived from digital topographic information in the form of slope, upstream drainage area, and planform curvature. The resulting CTI can be computed for each DEM raster grid cell and has been integrated into a geographical information systems (GIS) interface for use in agricultural watershed modeling tools (Momm et al., 2012; Bingner et al., 2010). The CTI is used to identify areas where gullies have high probability to form, including their most downstream locations.

Attributes can be computed from topographic representations such as point elevation, contour lines, raster grids, or triangular irregular network, with raster grid formats providing a widely used file format for hydrological applications. The quality of any analysis of topographic information depends on the quality of the digital elevation model (DEM) representation. DEM accuracy is a function of the spatial distribution of the original elevation data points, the interpolation method, and the selection of the raster grid cell size used to produce the DEM (Kienzle, 2004). The sampling interval and interpolation method both influence DEM accuracy (Aguilar et al., 2005; Ziadat, 2007). The relationship of raster grid cell size and topographic attributes devoted to hydrologic application has been extensively investigated. Zhang and Montgomery (1994) described how cumulative distributions of local slope (S), drainage area (A), and wetness index ($\ln(A/S)$), are affected by varying raster grid resolutions through analysis of two catchments with different relief characteristics. Slope was more influenced by resolution at locations with higher gradients and yielded lower average slope values as the raster grid resolution decreased. Average drainage area values increased as DEM resolution decreased, and average wetness index values increased as DEM resolution increased. These findings agree with the work of Kienzle (2004) for slope and wetness index. Kienzle (2004) also studied the effect of DEM resolution on profile and planform curvature and described an underestimation of these attributes as DEM raster grid cell size increased, prompting an underestimation of convergence and divergence areas.

In this study, the effect of overall terrain slope, local relief variance, and raster grid cell size on CTI values and cumulative distribution is investigated using both theoretical and observed catchment methodology. The theoretical analysis uses stochastic procedures of two-dimensional continuous random variables, or random fields (Isaaks and Srivastava, 1989), to generate simulated catchments and therefore quantify the influence of overall terrain slope, local relief variance, and raster grid cell size, each considered individually. In the observed analysis, study sites describing three distinct agricultural catchment areas with measured gully channel locations and high-resolution topographic information were selected to investigate the effect of overall terrain slope, relief variance, and raster grid cell size on CTI values. The findings from both analyses are discussed and reconciled in the Conclusions section.

MATERIALS AND METHODS

STUDY SITES

Three field-scale sites were selected for this study (fig. 1a). Site 1, referred to hereafter as KS, has an estimated drainage area of 6,969 m^2 and is located within the Cheney Lake watershed in Reno County, Kansas, which drains into Cheney Lake, the main source of drinking water for the city of Wichita, Kansas. Cheney Lake watershed has a total drainage area of 260,044 ha (642,584 acres) (Momm et al., 2012), and the predominant land use in this watershed is agriculture (>73%) in the form of cropland and rangeland. The study site was first topographically surveyed in 2008, and the gully channel thalwegs were measured using total station surveying equipment. In a second visit to the KS site, in March 2010, the ephemeral gully area was surveyed using a Topcon GLS-1000 series LiDAR scanner, which has a 2 mm single-point accuracy distance (Topcon, 2011). Although the soil was disturbed (i.e., tillage) between the first and second surveys, and slight differences in gully thalweg locations were observed, both gully channels were spatially very close to each other

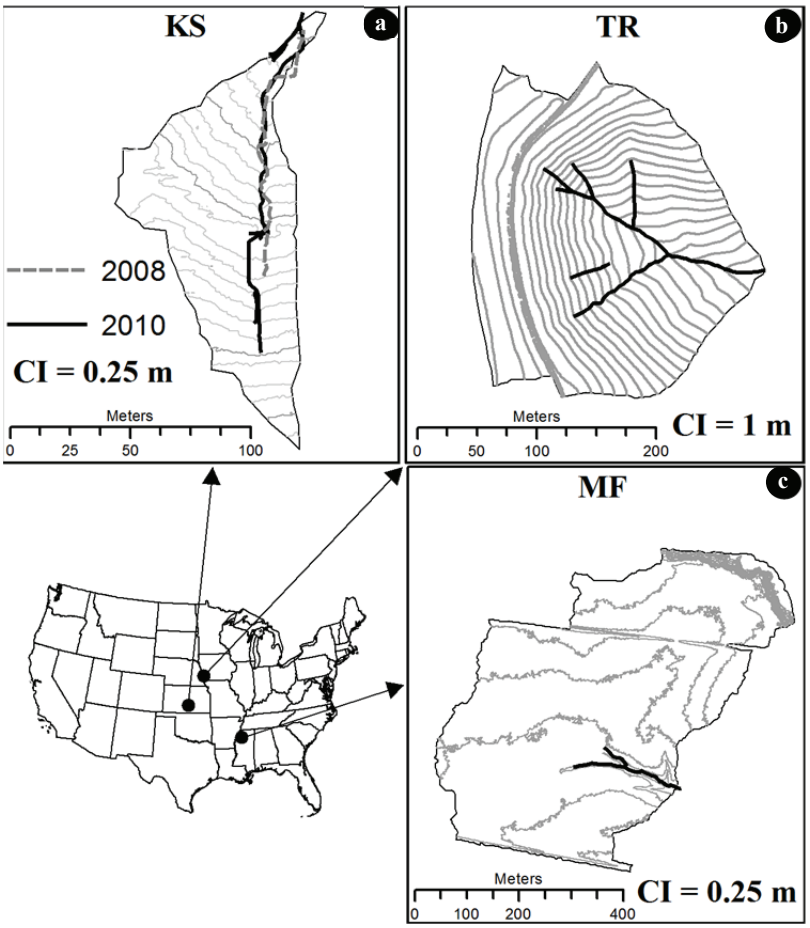

Figure 1. Agricultural fields used in the identification of zones prone to gully initiation. Dark lines represent measured gully channel thalwegs. Catchment boundaries and contour lines were generated from DEMs with 1 m raster grid cell size.

(fig. 1a). The second survey was composed of 11 individual LiDAR scans covering the extent of the gully channel, resulting in 945,668 laser points. From the high-resolution DEM generated from this survey, another channel thalweg location was determined (fig. 1a). The site was revisited a third time in November 2010, after the soil was disturbed with tillage. No gully was present at the time, and the entire site was surveyed using the same LiDAR scanner, producing 5,440,306 laser points from 17 independent scans. The survey conducted in November 2010 represented the entire contributing area of the gully investigated.

The second site, referred to hereafter as TR, has an estimated drainage area of 249,278 m^2 and is located at the USDA-ARS National Soil Tilth Laboratory Deep Loess Research Station near Treynor, Iowa (fig. 1b). The TR site consists of slopes ranging from 2% to 4% at the ridges and valleys and from 12% to 16% for mid-slopes (Rachman et al., 2008). DEMs for this site were generated from an airborne LiDAR survey performed in 2008, and the gully locations were obtained from Renard et al. (1997). This watershed is composed of highly erodible soils (silt loam, fine-silty, and mixed) prone to forming gullies (Karlen et al., 2009; Rachman et al., 2008).

The third site, referred to hereafter as MF, has an estimated drainage area of 49,498 m^2 and is located within the Yazoo River basin in northwestern Mississippi (fig. 1c) and was in continuous row crop cultivation. Producers have modified the field topography using laser-guided leveling and the installation of a drainage network in the form of ditches (Shields et al., 2011). DEMs for this site were generated from an airborne LiDAR survey, and gully location was surveyed by total station equipment.

THEORETICAL EVALUATION

Generation of Simulated Catchments

The effect of terrain characteristics and DEM resolution on CTI values and distribution was investigated through the use of probabilistic random functions (Holt et al., 2003). Two-dimensional regularly spaced grids (1024 rows × 1024 columns) were populated with simulated elevation residual values (deviations from local mean elevation) randomly generated using spectral and fast Fourier transform (FFT) methods (fig. 2a). Multiple independent realizations were performed using the microsecond part of the computer clock as seed for the random number generator. These generated values are influenced by the selected cumulative distribution function and the respective mean and variance values that describe the distribution. Two intermediate raster grids were generated by adding surface planes to the raster grid containing the elevation residual values: (1) adding two sloping inward planes

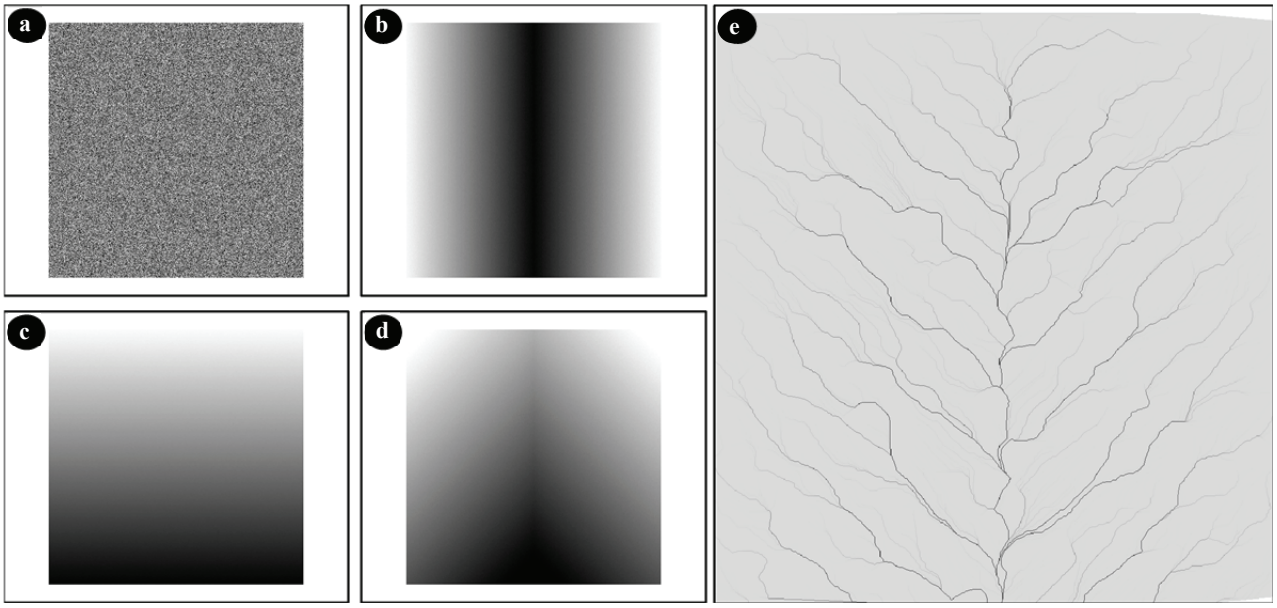

Figure 2. Steps performed for theoretical investigation of the effect of topographic characteristics on CTI. A random field with mean 0.0 and varying variance (a) was added to two planar surfaces sloping inwards (b) and to a planar surface sloping downward on the page (c). The two resulting surfaces were then added to form a simulated catchment area (d). From the simulated catchment area, different topographic attributes were computed, such as the concentrated flow path (e).

(fig. 2b), and (2) adding a single sloping downward plane (fig. 2c). The two intermediate raster grids were combined to form one simulated catchment raster grid (fig. 2d). Using standard topographic analysis tools, topographic attributes were calculated for the raster grid (fig. 2e). The variance describing the cumulative distribution and slope of the surface planes was used to describe local elevation variations (surface roughness) and overall catchment terrain slope, respectively.

The topographic survey from the KS measured field (i.e., "real world") was selected to examine observed elevation residual distributions due to the detailed topographic information generated from the terrestrial-LiDAR survey. Intermediate raster grids were generated using moving average kernels of varying window sizes (5×5, 7×7, 9×9, 11×11, 13×13, 15×15, 17×17, 19×19, and 21×21 cell size) to filter the elevation raster grid. Elevation residual grids were obtained by subtracting the measured elevation grid from the intermediate filtered raster grids. For each window size, the elevation residuals were plotted against normal frequency of occurrence to observe the shape of the distribution. From this analysis, a bell-shaped cumulative distribution function (fig. 3) was selected for use in the simulated catchment generation.

The influences of terrain roughness, terrain overall slope, and raster grid cell size on CTI values and distribution were evaluated individually. A set of simulated catchments was generated to evaluate each variable considered (table 1). For the evaluation of the influence of terrain roughness on CTI, elevation residual raster grids were generated using constant mean and varying variance. For each variance value considered, 20 independent realizations were performed, resulting in a total of 200 elevation residual raster grids. A surface plane with slope of 0.05 m m^{-1} was combined with the elevation residuals in the generation of the final catchments used in this evaluation. The influence of overall terrain slope on CTI values was evaluated in a similar fashion. A set of ten elevation residual raster grids was generated using constant mean and variance values. These elevation residual grids were added to surface planes with varying overall slope values. This procedure yielded a total of 120 simulated catchments.

For the evaluation of the influence of raster grid size on CTI values, a slightly different procedure was investigated. Ten reference catchments were independently generated with constant mean and variance values and surface plane slope values (table 1). For each of the ten reference catchments, a set of points was randomly selected from the uniformly distributed grid and assigned the elevation value of the raster cell they fell into. Each set of points was interpolated into continuous raster grids having a factor resolution (1, 1/2, 1/4, 1/8, and 1/16) of the original resolution (fig. 4). A range of uniformly distributed random points between 500 and 2500 was tested; 1500 points was selected to be the balance value that yielded a manageable number of points while generating an interpolated raster grid that closely represented the original raster grid. For instance, an interpolated grid with a factor of 1 times the original resolution generated a raster grid that had the same spatial resolution as the original simulated catchment field of 1024 rows × 1024 columns, while a factor of 1/16 times the original resolution generated a raster grid with 64 rows × 64 columns for the same spatial extent. The continuous surfaces were generated using the piecewise cubic curvature-minimizing interpolation algorithm implemented in the Scientific Python library (Nielson, 1983; Renka and Cline, 1984). Different interpolation algorithms could have been employed; however, the effect of various interpolation algorithms on DEM accuracy, and therefore on CTI values, is beyond the scope of this study.

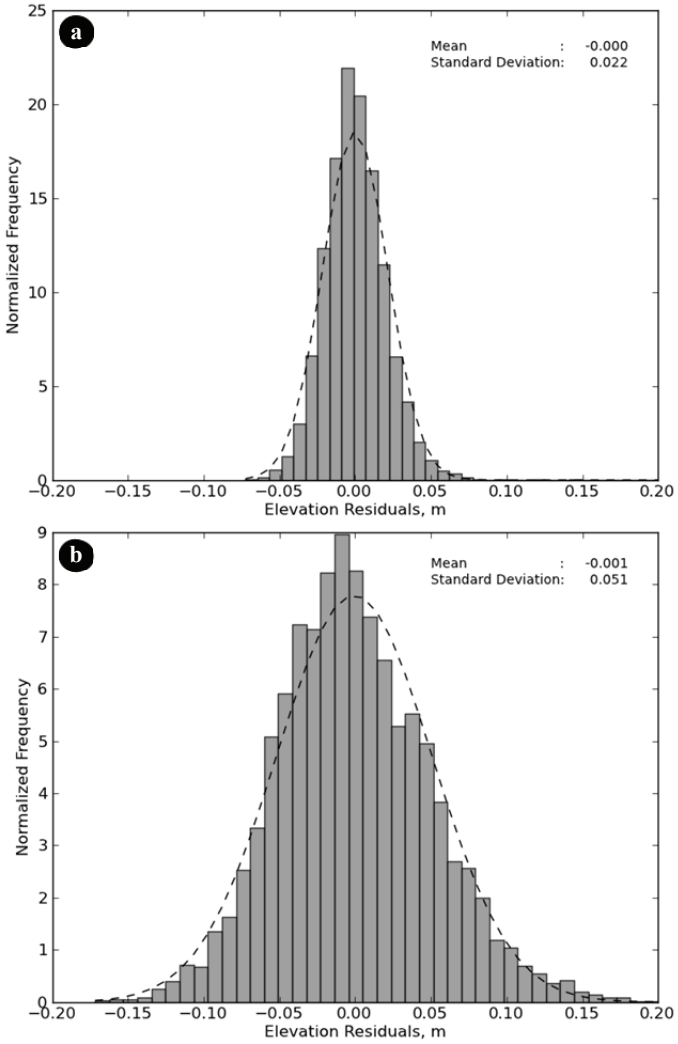

Figure 3. Comparison of surface elevation residual distribution with a corresponding normal distribution. Subtracting the measured surface from a smoothed surface using different kernel sizes (5×5 in a and 21×21 in b) generated the residuals surfaces.

The interpolation method described here to obtain continuous raster grids from irregularly spaced spot points was chosen to better represent practical DEM raster grid generation (i.e., continuous grids from point clouds obtained using terrestrial LiDAR surveys) over the alternative method of resampling the raster grid with higher resolution into different lower-resolution raster grids. For each simulated catchment area, ten replications (random generation of spot locations for each resolution considered) were performed, yielding a total of 500 simulated catchment fields (10 random field realizations × 10 replications × 5 resolutions).

Table 1. Parameters used in the generation of simulated catchments.

		Variables Investigated		
Parameter	Parameter Description	Terrain Roughness	Overall Slope	Raster Grid Size
1	Mean of reference distribution	0.0	0.0	0.0
2	Variance of reference distribution	0.05, 0.10, 0.15, 0.20, 0.25, 0.30, 0.35, 0.40, 0.45, and 0.50	0.05	0.05
3	Reference grid cell size	1024×1014	1024×1024	1024×1024
4	Number of reference grids generated for each variance value (realizations)	20	20	10
5	Plane slope values	0.05 m m^{-1}	0.01, 0.05, 0.10, 0.15, 0.20, and 0.25 m m^{-1}	0.05 m m^{-1}
6	Number of sets of spot elevation points	N/A	N/A	10
7	Interpolated grid cell size	N/A	N/A	1024, 512, 256, 128, and 64
8	Total number of simulated catchments	200[a]	120[b]	500[c]

[a] 10 variance values (parameter 2) × 20 realizations (parameter 4).
[b] 20 realizations (parameter 4)× 6 overall slope values (parameter 5).
[c] 10 realizations (parameter 4) × 10 sets of spot points (parameter 6) × 5 grid sizes (parameter 7).

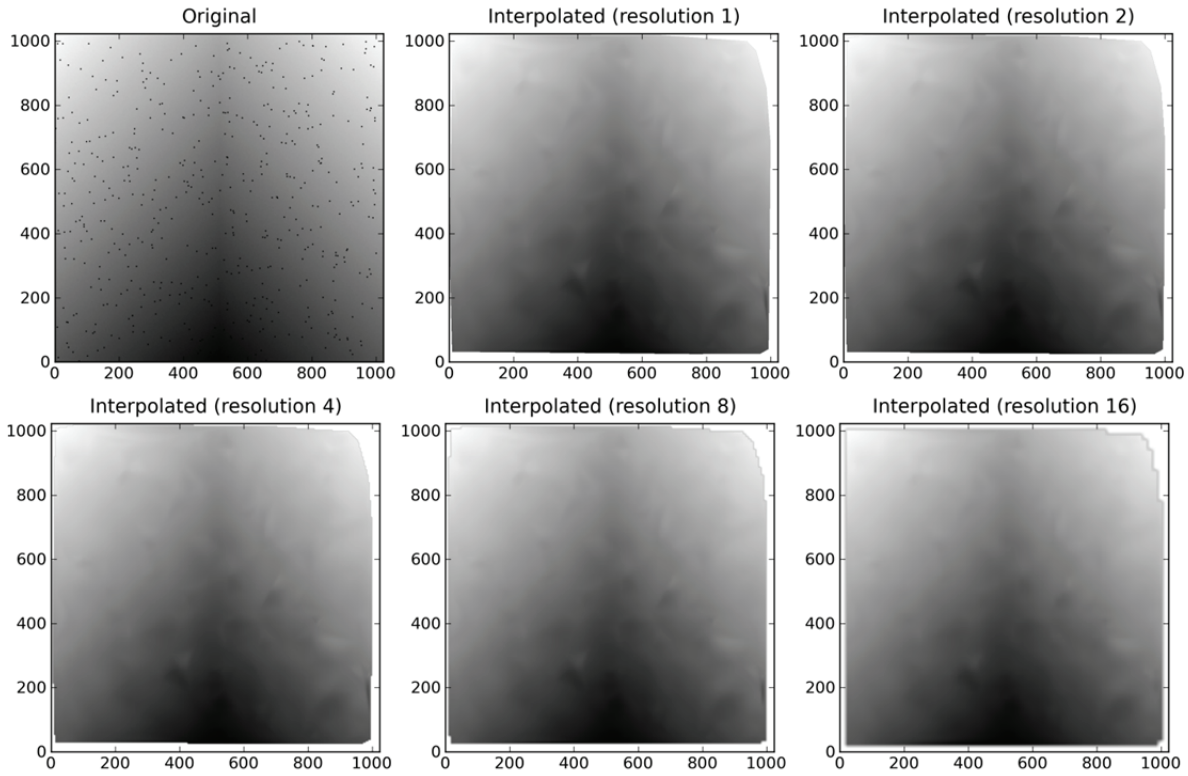

Figure 4. Procedure for evaluation of raster grid cell size effect on CTI values. Random spot locations were selected to derive elevation from the random field and then interpolated to different raster grid cell sizes.

Topographic Attributes

Preprocessing simulated catchment areas to generate the required topographic attributes for the CTI analysis was performed using the topographic parameterization (TOPAZ) computer program (Garbrecht and Martz, 1996, 1997). Examples of topographic attributes include slope, aspect, flow direction, and flow accumulation. For each simulated catchment (simulated raster grid), TOPAZ was used twice. The primary objective of the first run was to obtain the catchment outlet location, while the second run was used to compute local slope, flow accumulation, flow direction, and catchment boundary.

In the first run, TOPAZ was run in reduced mode (DEM preprocessing only) to remove small imperfections in the data, such as filling small sinks to improve the subsequent determination of flow direction and flow accumulation raster grids. The resulting flow accumulation raster grid, from the first run, was used with an automated algorithm to determine the row and column of the raster grid cell representing the catchment outlet. The raster grid row representing the outlet of the catchment was fixed so that all catchments resulting from the hydrological analysis would have roughly the same size (except when the identified outlet location was a junction of two or more flow paths, causing the next downstream row to be used instead). No smoothing or resampling of the simulated raster grids was performed.

The second run of the TOPAZ computer program was used to compute local slope, flow accumulation, flow direction, and catchment boundary. The contributing area was computed using the flow accumulation grid and the raster grid cell size. Planform curvature raster grids were generated using the method described by Zevenbergen and Thorne (1987), and the CTI raster grids were calculated according to Thorne et al. (1986) by:

$$\mathrm{CTI} = A^{*}S^{*}PLANC \tag{1}$$

where A is upstream drainage area (m^2), S is the local slope ($m\ m^{-1}$), and $PLANC$ the planform curvature (1/100 m).

Normalization of CTI Distribution

Only the resulting positive CTI values were considered as possible locations for gully initiation, since negative values are the result of negative planform curvature (ridges). The set of positive CTI values exhibited, roughly, a log-normal distribution shape, but variations in topographic characteristics (relief variance, overall slope, and DEM resolution) yielded distinct distributions. In an attempt to standardize different distributions and to provide for easier comparison between catchments, each distribution was normalized using:

$$\mathrm{CTI}_n = \frac{\log_{10}(\mathrm{CTI}) - \mu}{\sigma},\ \forall\ \mathrm{CTI} > 0 \tag{2}$$

where μ and σ are the mean and variance of $\log_{10}$(CTI) values, respectively.

Table 2. Summary statistics of topographic information for the three sites investigated.

Site[a]	Minimum Elevation (m)	Maximum Elevation (m)	Average Elevation (m)	Standard Deviation of Residuals[b]	Average Overall Slope[b] (m m^{-1})	Drainage Area at Outlet[b] (m^2)	Average Nearest Neighbor Distance (m)
KS	495.84	503.54	498.64	0.014	0.030	6,969	0.035
TR	351.02	373.47	363.38	0.025	0.100	249,278	0.901
MF	53.18	63.81	56.36	0.020	0.002	49,486	0.620

[a] KS = observed catchment within the Cheney Lake watershed in Reno County, Kansas; TR = observed catchment near Treynor in Pottawattamie County, Iowa; and MF = observed catchment in the Yazoo River basin in Tunica County, Mississippi.
[b] Calculated from the interpolated raster grid at 1 m resolution.

OBSERVED CATCHMENT EVALUATIONS

Topographic Representation

Raster grids for the three observed study sites (KS, TR, and MF) were generated at varying raster grid cell sizes of 1, 2, 4, and 8 m by interpolating point clouds using the inverse distance weighted algorithm (de Berg et al., 2000), implemented in the LP360 software package (QCoherent, 2011), that considers ten nearest neighbors and a power of 2. Table 2 lists descriptive statistics for the three study sites. Minimum elevation, maximum elevation, average elevation, and average nearest neighbor distance were computed from the point clouds, while the standard deviation of elevation residuals and average overall slope were determined from the 1 m interpolated raster grid. The standard deviation of elevation residuals was computed using the Daubechies 2D discrete wavelet decomposition method, available in the discrete wavelet transform in Python (PyWavelets, 2011). Overall slopes were calculated over multiple cross-sections at different orientations and then averaged.

Identification of Critical CTI Values

Measured gully channel thalweg locations were used as reference datasets to evaluate the effectiveness of using CTI as a proxy for unit stream power in mapping locations prone to gully initiation. For each site and for each raster grid resolution considered, raster grids containing the distance of the cell to the closest location of the channel thalweg were generated (fig. 5). Field observations at the KS study site indicated that the gully main channel forms at slightly different locations each season based on furrow alignment. A buffer distance of 5 m in either direction from the measured channel thalweg was defined as the buffer zone. The distance raster grid was then used to assign a class to each predicted location as either in agreement with or not in agreement with measured gully information. If the distance of the predicted location was less than the buffer zone (5 m), the predicted location was assigned to the inside class (in agreement with). Otherwise, the predicted location was assigned to the outside class (not in agreement with).

Maps of positive CTI values (negative values were excluded) were generated and clipped to the catchment area boundaries. The positive values were then sorted from smallest to largest and summarized by calculating the cumulative distribution function. Binary maps were then created through a process that assigned 1 to values greater than the user-defined threshold, and zero otherwise. The raster grid cells with values of 1 were then further classified into inside or outside based on comparison with the gully channel buffer zone. An iterative procedure varying the user-defined threshold was used to identify the critical CTI value (user-defined threshold) that would maximize the number of points located within the buffer zone (assigned inside) while minimizing the occurrence of raster grid cells outside the buffer zone (assigned outside). The number of inside and outside assigned raster grid cells was recorded, and the proportion of difference between the number of inside (N_{inside}) and outside ($N_{outside}$) points was computed using:

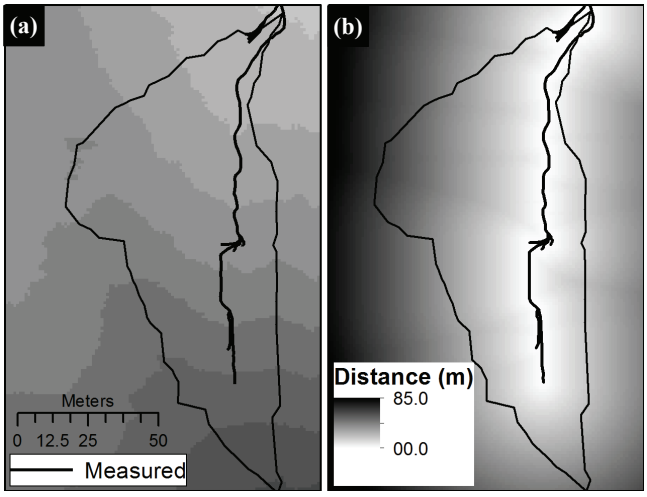

Figure 5. Illustration of vectors and raster grid features used as reference for evaluation of the CTI threshold procedure in identifying gully initiation locations. The measured gully thalweg location for the KS site (dark polyline in a and b) was used to generate a distance raster grid (raster grid in b), where each raster grid cell is assigned a value corresponding to the distance to the closest segment of the gully channel thalweg.

$$\mathrm{P}\ (\%) = \frac{N_{inside} - N_{outside}}{N_{inside} + N_{outside}} \tag{3}$$

The entire procedure was repeated for each cumulative percentage threshold by adding 0.01% to the previous cumulative percentage threshold until either no points were identified or the value of 100% was reached. An example of the proportion of difference between inside and outside points for the KS site at a 1 m raster grid cell size is shown in figure 6. The critical CTI value was defined as the point on the curve with the highest number of points above CTI threshold (i.e., peak value).

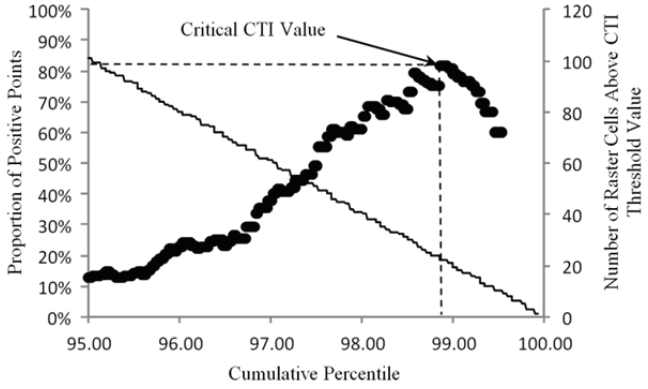

Figure 6. Black dots represent the critical CTI value, and the continuous line represents the number of raster grid cells with CTI values above the critical CTI value. As the CTI threshold value increases, the number of raster grid cells above that value decreases. The critical CTI value was defined as the segment of the curve with the highest proportion value and with the maximum number of points.

RESULTS AND DISCUSSION

THEORETICAL EVALUATION

Simulated watersheds provided the necessary information for analyses that isolated and led to evaluations of various individual topographic characteristics. Varying the variance describing the distribution used in the random field procedure, as a proxy for relief variance or terrain roughness, indicated a small variation in contributing area at the outlet (fig. 7a). Analysis of the top 0.1% of CTI values revealed a steady increase in average CTI values as the terrain becomes rougher (fig. 7d). A 10-fold increase in terrain roughness resulted in a 7.5-fold increase in the average top 0.1% CTI values. This can be partially attributed to the influence of relief variance on local slope (fig. 7b) and planform curvature (fig. 7c). Rougher terrains will, on average, yield higher local slope values and change the planform curvature distribution. Similarly, varying the overall watershed slope had little effect on the drainage area at the outlet (fig. 8a) and increased the local slope (fig. 8b) (as reported by Zhang and Montgomery, 1994), planform curvature (fig. 8c), and top 0.1% CTI values (fig. 8d). Changes were more pronounced when varying raster grid cell sizes (fig. 9). As raster grid cell size increased, local slopes (fig. 9b) and planform curvature (fig. 9c) decreased, matching similar findings by Kienzle (2004) and Zhang and Montgomery (1994). The main change was found in the average top 0.1% CTI values, which demonstrated an inverse power function behavior of the following form, with r^2 of 0.82:

$$\text{Mean top 0.1\% CTI} = 263{,}466.87(\text{DEM}_{\text{resolution}})^{-0.7} \quad (4)$$

Different DEM resolutions can yield CTI values that

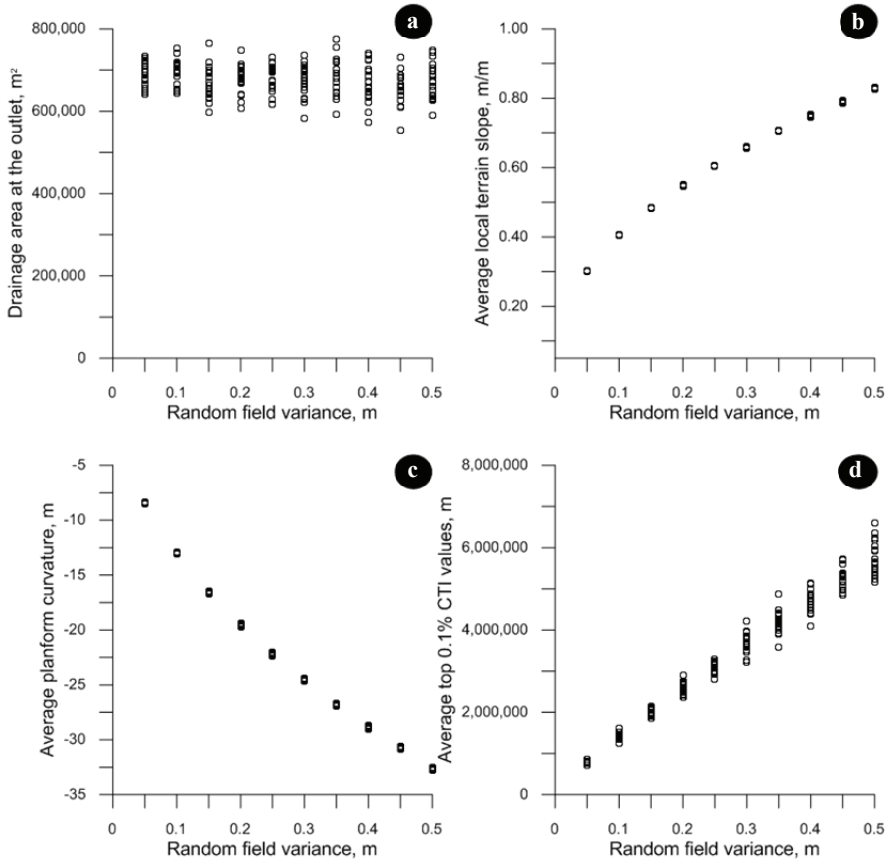

Figure 7. Results of theoretical investigation of the effect of terrain roughness (represented by the variance elevation residuals used to generate simulated catchments) on CTI: (a) drainage area at the outlet of the field, (b) average local terrain slope within the catchment area, (c) average planform curvature within the catchment area, and (d) average of top 0.1% CTI values. Results were generated considering 20 random field realizations.

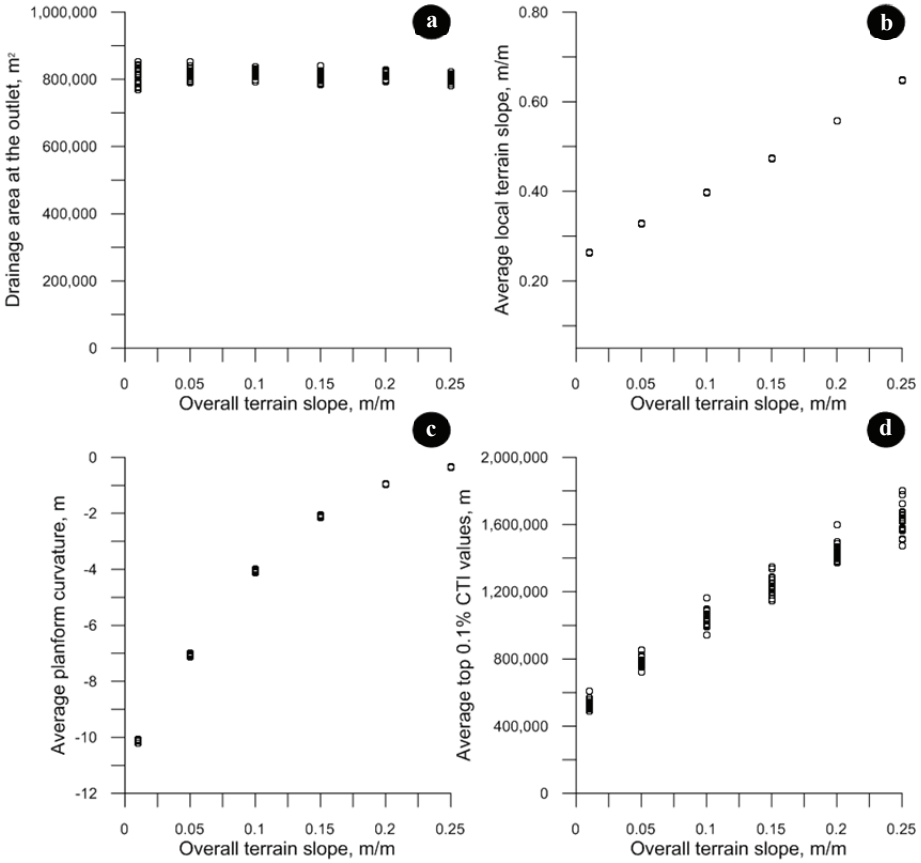

Figure 8. Results of theoretical investigation of the effect of overall terrain slope on CTI: (a) drainage area at the outlet of the field, (b) average local terrain slope within the catchment area, (c) average planform curvature within the catchment area, and (d) average of top 0.1% CTI values. Results were generated considering 20 random field realizations.

vary over many orders of magnitude, limiting comparisons between different studies and leading to lack of standardization. The effect of topographic characteristics and raster grid cell size on CTI values was also observed in cumulative distribution function plots (fig. 10). The logarithm of cumulative frequency of CTI values indicated that an increase in terrain variance caused a shift of the cumulative distribution curves while maintaining relative slope. This can be verified by changes in median CTI values from 1.6 (random field variance of 0.05) to 2.210 (random field variance of 0.5), while the interquartile range remained constant at approximately 1.1 (fig. 10a). Conversely, as the catchment overall slope increased, the cumulative distribution changed in both mean and variance (curve shift and slope change). Median CTI values ranged from 1.3 to 2.2, and the interquartile range varied from 1.1 to 1.6, for simulated catchments with overall slopes of 0.01 and 0.25 m m^{-1}, respectively (fig. 10c). In addition to changes in mean and variance, the variation in raster grid cell size also introduced changes to the shape of the overall cumulative distribution curve of the logarithm CTI (figs. 10g and 10h). Results suggest that simulated interpolated catchments changed the cumulative distribution curve shape from a normal distribution to a tri-modal distribution. Different interpolation techniques were evaluated, and similar changes in histogram shape were observed. The multi-modal distribution was more accentuated for the higher-resolution raster grids than for lower-resolution raster grids.

The effects of random field variance and overall terrain slope on CTI distribution was significantly reduced (figs. 10b and 10d) by normalizing CTI using log base 10, the mean, and standard deviation (eq. 2). The effect of DEM resolution on CTI distribution was reduced to a lesser extent as different resolutions yielded different distribution shapes (fig. 10f). Normalized CTI cumulative distribution curves of the random field variance investigation yielded median values ranging from 0.02 (random field variance of 0.05) to 0.05 (random field variance of 0.5) and interquartile range values of approximately 0.88. Similarly, the distribution analysis for overall slope variation using normalized CTI values generated median values ranging from 0.0047 to -0.0953 and interquartile range values of 0.87 to 1.23 for the cases with overall slopes of 0.01 and 0.25 m m^{-1}, respectively.

Observed Catchment Evaluation

The three observed watersheds have distinct topographic characteristics in terms of relief variance, overall slope, and drainage area size. Analysis of the effect of variations in DEM spatial resolution on CTI values indicated similar findings as the theoretical investigation. As the raster grid cell size increased, small variations in drainage area at the

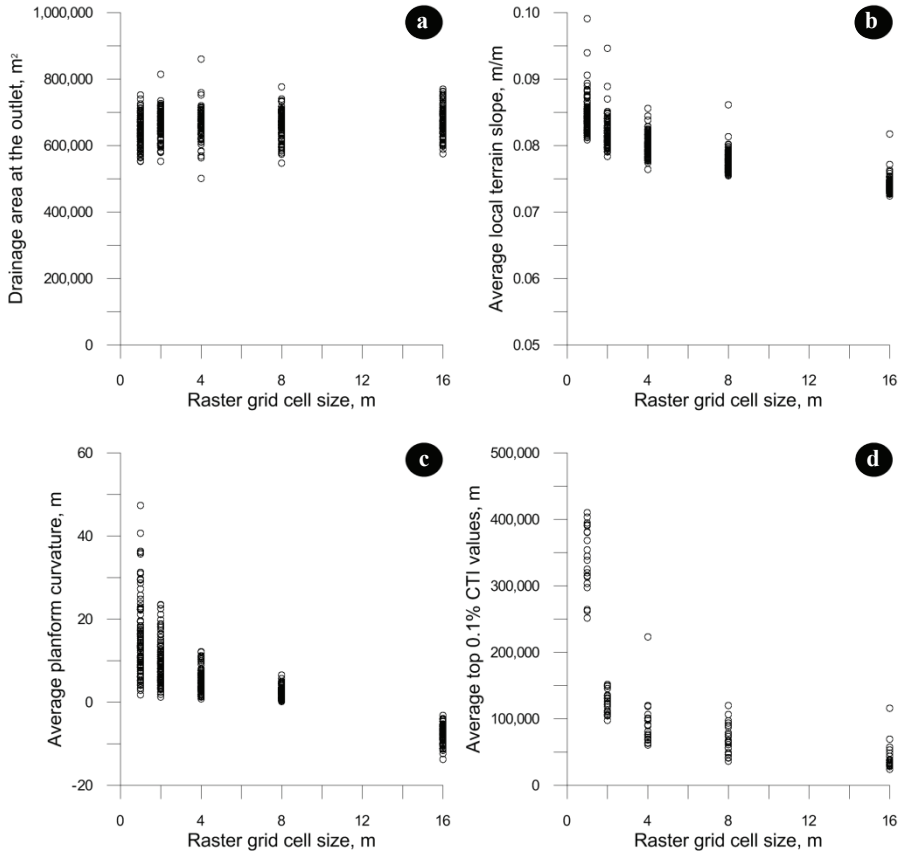

Figure 9. Results of theoretical investigation of the effect of raster grid resolution on CTI values: (a) catchment area at the outlet of the field, (b) average local terrain slope within the catchment area, (c) average planform curvature within the catchment area, and (d) average of top 0.1% CTI values. Results were generated considering ten realizations for random field generation with ten repetitions of random sampling for interpolation of DEMs at six different resolutions.

catchment outlet were observed (fig. 11a). Average local slopes decreased (fig. 11b), and average planform curvature increased toward zero (fig. 11c), indicating that DEMs generated at higher raster grid sizes have a limited ability to detect topographic variations smaller than the raster grid cell size. This reduced ability to capture small topographic changes was also reflected in the average top CTI values, which, similar to the simulated datasets, demonstrated a reverse power function behavior (fig. 11d).

Comparisons of cumulative distribution functions for the three observed sites at different resolutions are depicted in figure 12. Similar to the simulated results, CTI cumulative values for higher-resolution grids tended to have multi-modal logarithmic distributions, while lower resolutions were closer to log-normal distributions (fig. 12, first column). This effect was more pronounced for the observed KS field. Normalization of these distributions was more effective in merging different distribution curves at lower resolutions (4 and 8 m), resembling the theoretical investigation.

Identification of critical CTI values based on measured gully channel locations revealed a wide range of possible values (table 3). Maps of spatial distribution of raster grid cells with values greater than or equal to the selected critical CTI values indicate a good agreement with measured data (fig. 13). Critical CTI values varied between fields, influenced mainly by the differences in catchment drainage areas. Additionally, critical CTI values were influenced by raster grid spatial resolution, as the CTI values varied within fields by many orders of magnitude. Normalization of positive CTI values reduced the influence of drainage area on CTI values, allowing for better comparisons between sites. Although variations between sites and within sites with different resolution still yielded different critical CTI_n values, results indicate a reduction in the range of possible critical values. For example, for a 1 m spatial resolution, the original critical CTI value for MF is approximately 57 times larger than the critical CTI value for KS, but the critical CTI_n value for MF is only 1.8 times larger than the critical CTI_n value for KS.

CONCLUSIONS

The objectives of this study were to describe the effect of different topographic characteristics on CTI distribution and to evaluate normalization procedures for CTI values to support improved identification of watershed zones prone to ephemeral gully initiation. Results indicate that CTI values and their corresponding distributions are both influenced by topographic characteristics (terrain variance and overall slope) and raster grid cell size in different ways. Increases in relief variance (a proxy descriptor of surface roughness) and overall catchment slope both tend to yield higher CTI

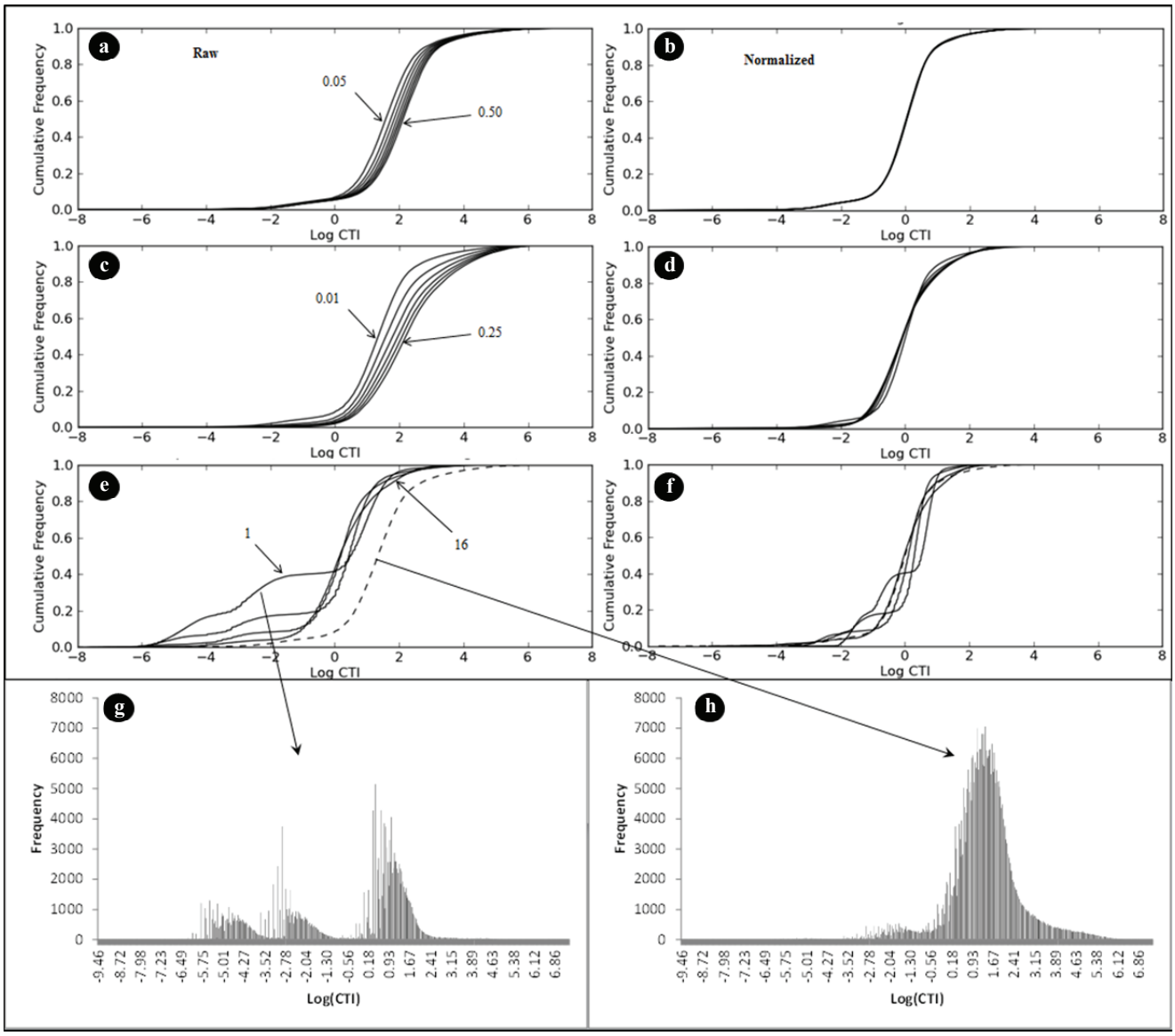

Figure 10. Cumulative distribution functions of logarithm of positive raw and normalized CTI values as (a and b) terrain variance, (c and d) terrain overall slope, and (e and f) raster grid cell size varied. Dashed lines in plots e and f represent the simulated surface at the original resolution at which the random field was generated (no interpolation performed). Histograms for the interpolated watershed at the same resolution as (g) the random field and (h) the simulated surface with no interpolation illustrate the differences in distribution shape.

values in response to variations in local slope and planform curvature. Normalization of cumulative distribution functions of $\log_{10}$(CTI) for positive CTI values produced matching distribution curves when relief variance and overall slope varied. This finding may be seen as a possible alternative for investigations of large watersheds with more than one topographic characteristic, which are traditionally addressed by identifying a critical CTI value for each topographic characteristic. The normalization procedure had a lesser effect on variations in raster grid cell sizes, as the overall distribution shape was different at multiple raster grid cell sizes. However, the normalization procedure improved comparisons between different sites with distinct drainage area sizes and topographic characteristics.

The determination of critical CTI_n values through comparison to measured gully thalweg yielded unique values as resolution and fields varied. Discrepancies in critical CTI_n values in the same catchment field due to changes in raster grid cell size were significantly reduced when compared to the original CTI values, although not fully eliminated. This may be attributed to the inherent limitations of the raster grid representation at lower resolutions acting as smoothing filters, leading to reduced topographic information. Critical CTI_n values for different fields represented at the same DEM raster grid cell size also differed. This may be attributed to differences in physical properties other than topographic, as the occurrence of gullies depends on a wide range of physical (soil properties, precipitation pattern, etc.) and management practices in addition to topographic parameters.

Understanding the effect of topographic characteristics and DEM raster grid cell size on critical CTI values is essential for developing automated techniques to locate

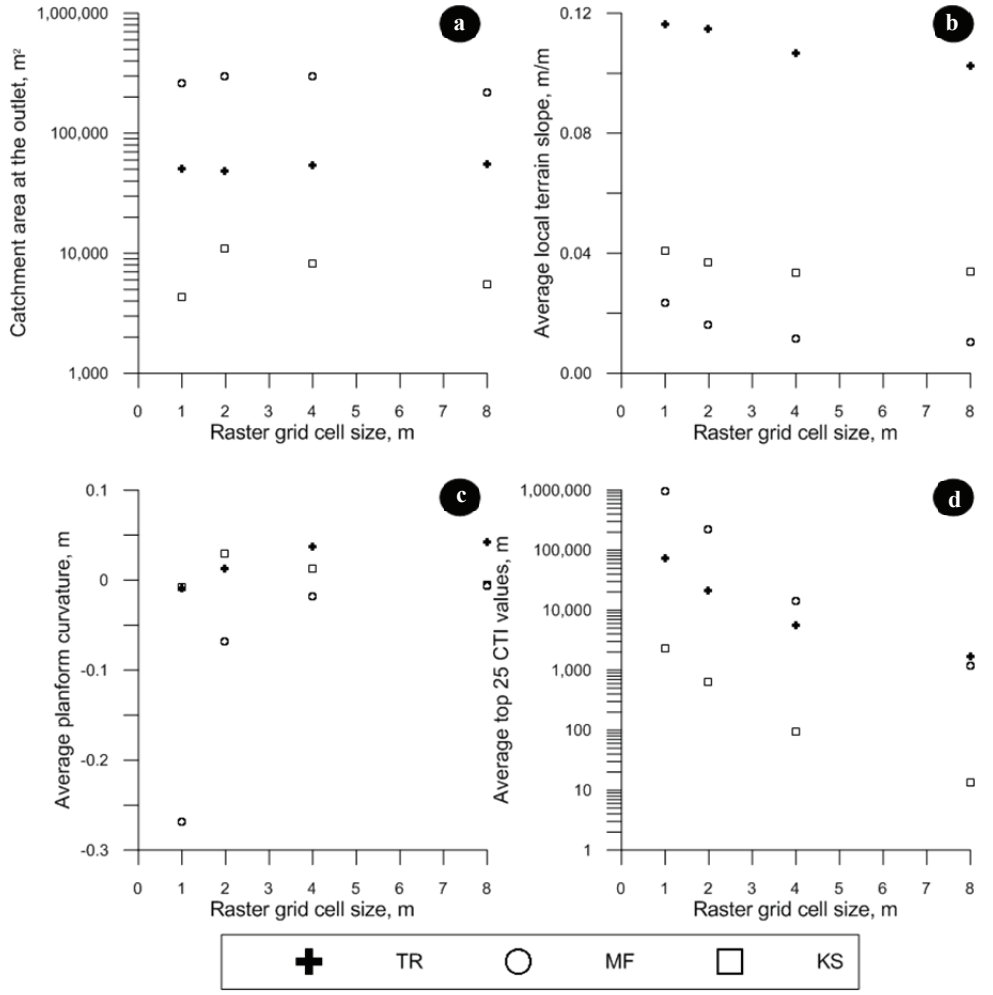

Figure 11. Comparison of topographic attributes for the three catchments evaluated. Variations in (a) catchment drainage area at the outlet, (b) average slope, (c) average planform curvature, and (d) top 25 CTI values are plotted against the four raster grid cell sizes considered.

gully initiation points that can be used in technologies to assess the effect of conservation practices in agricultural watersheds. Results indicate that the proposed normalization method reduced the influence of topographic characteristics on critical CTI_n values, allowing for comparisons between sites represented at similar spatial resolution. These findings suggest that a normalized critical CTI between 1 and 2 could be used for the identification of areas with high potential for gully initiation, supporting targeted conservation and mitigation efforts to promote sustainable agriculture.

Future investigations into methodologies using the stream power concept (based on topographic attributes to identify areas prone to gully initiation) should focus on improved topographic representation and incorporation of soil properties into the decision-making process. Improved surveying techniques using airborne and ground LiDAR generate irregularly spaced point clouds with uneven distribution of points. Interpolation of these point clouds into regular grids introduces uncertainty and reduces topographic information in areas with a high point density, but does not add additional information in areas with low point density. A possible alternative for the uneven distribution of points would be the development of technology to represent and process topographic information using irregular grids, such as triangular irregular networks. Furthermore, gully initiation is driven by a combination of different physical features, in which soil characteristics play an important role. The incorporation of soil properties in the determination of critical CTI values should improve the overall

Table 3. Comparison of critical CTI values for the three catchments.

Site[a]	Resolution (m)	Percentile (%)	CTI	log(CTI)	CTI_n
KS	1	98.87	1,327.9	3.12	1.52
	2	96.49	113.6	2.05	1.12
	4	88.64	45.2	1.66	1.02
	8	79.25	11.2	1.05	0.59
TR	1	99.87	38,916.4	4.59	2.06
	2	99.06	6,342.9	3.80	1.93
	4	97.24	1,342.3	3.13	1.80
	8	95.21	879.2	2.94	1.72
MF	1	99.92	75,044.1	4.87	2.67
	2	99.89	37,313.0	4.57	2.38
	4	99.53	1,412.4	3.14	1.83
	8	98.62	200.7	2.30	1.58

[a] KS = observed catchment within the Cheney Lake watershed in Reno County, Kansas; TR = observed catchment near Treynor in Pottawattamie County, Iowa; and MF = observed catchment in the Yazoo River basin in Tunica County, Mississippi.

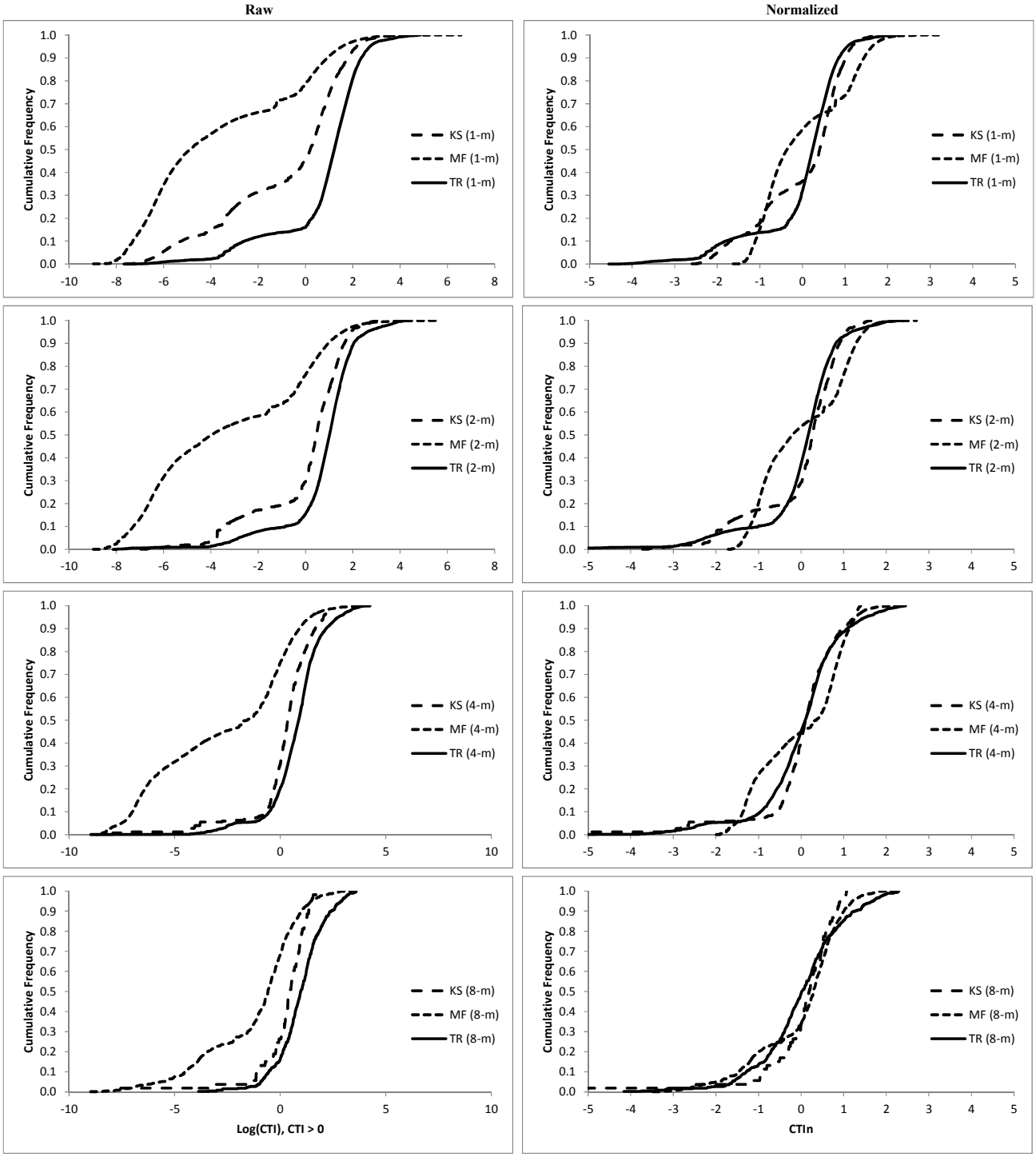

Figure 12. Cumulative distribution functions of standardized variable of logarithm of positive CTI values for the three watersheds investigated at different raster grid cell sizes.

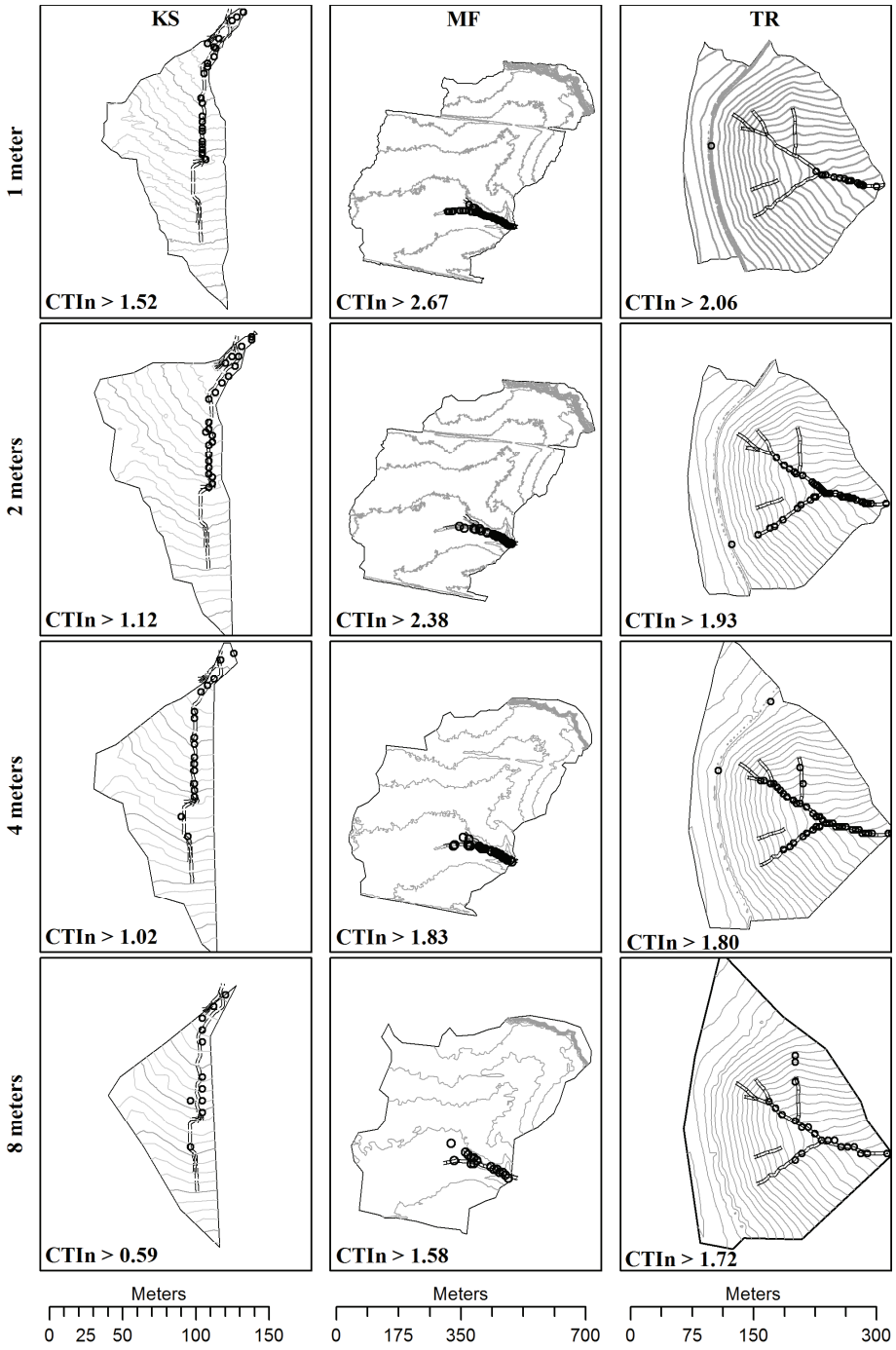

Figure 13. Spatial distribution of locations with CTI_n larger than or equal to critical CTI_n values.

accuracy of the procedure, as different soils respond differently to erosion based on their physical characteristics.

REFERENCES

Aguilar, F. J., F. Aguera, M. A. Aguilar, and F. Carvajal. 2005. Effects of terrain morphology, sampling density, and interpolation methods. *Photogram. Eng. and Remote Sens.* 71(7): 805-816.

Bingner, R. L., and F. Theurer. 2001. AGNPS 98: A suite of water quality models for watershed use. In *Proc. 7th Federal Interagency Sedimentation Conf.* Reston, Va.: U.S. Geological Survey.

Bingner, R. L., R. R. Wells, H. G. Momm, F. D. Theurer, and L. D. Frees. 2010. Development and application of gully erosion components within the USDA AnnAGNPS watershed model for precision conservation. In *Proc. 10th Intl. Conf. on Precision Agric*. Denver, Colo.: Colorado State University.

de Berg, M., M. van Kreveld, M. Overmars, and O. Schwarzkopf. 2000. *Computational Geometry: Algorithms and Applications*. 2nd ed. Berlin, Germany: Springer-Verlag.

Garbrecht, J., and L. W. Martz. 1996. Digital landscape parameterization for hydrological applications. In *HydroGIS 96: Application of Geographic Information Systems in Hydrology and Water Resources Management*, 169-174. IAHS Publ. No. 235. International Association of Hydrological Sciences.

Garbrecht, J., and L. M. Martz. 1997. The assignment of drainage direction over flat surfaces in raster digital elevation models. *J. Hydrol.* 193(1): 204-213.

Gordon, L. M., S. J. Bennett, C. V. Alonso, and R. L. Bingner. 2008. Modeling long-term soil losses on agricultural fields due to ephemeral gully erosion. *J. Soil and Water Cons*. 63(4): 173-181.

Holt, R. M., R. J. Glass, J. M. Sigda, and E. D. Mattson. 2003. Influence of centrifugal forces on phase structure in partially saturated media. *Geophysical Res. Letters* 30(13): 1692, doi: 10.1029/2003GL017340.

Isaaks, E. H., and R. M. Srivastava. 1989. *An Introduction to Applied Geostatistics*. New York, N.Y.: Oxford University Press.

Karlen, D. L., D. L. Dinnes, M. D. Tomer, D. W. Meek, C. A. Cambardella, and T. B. Moorman. 2009. Is no-tillage enough? A field-scale watershed assessment of conservation effects. *J. Integrative Biosci.* 7(2): 1-24.

Kienzle, S. 2004. The effect of DEM raster resolution on first order, second order, and compound terrain derivatives. *Trans. in GIS* 8(1): 83-111.

Mitasova, H., J. Hofierka, M. Zlocha, and L. Iverson. 1996. Modeling topographic potential for erosion and deposition using GIS. *Intl. J. Geograph. Info. Syst.* 10(5): 629-641.

Momm, H. G., R. L. Bingner, R. R. Wells, and D. Wilcox. 2012. AGNPS GIS-based tool for watershed-scale identification and mapping of cropland potential ephemeral gullies. *Applied Eng. in Agric.* 28(1): 1-13.

Montgomery, D. R., and W. E. Dietrich. 1992. Channel initiation and the problem of landscape scale. *Science* 255(5046): 826-830.

Moore, I. D., and G. J. Burch. 1986. Modeling erosion and deposition: Topographic effects. *Trans. ASAE* 29(6): 1624-1630.

Moore, I. D., G. J. Burch, and D. H. Mackenzie. 1988. Topographic effects on the distribution of surface soil water and the location of ephemeral gullies. *Trans. ASAE* 31(4): 1098-1107.

Moore, I. D., R. B. Grayson, and A. R. Ladson. 1991. Digital terrain modeling: A review of hydrological, geomorphological, and biological applications. *Hydrol. Proc.* 5(1): 3-30.

Nielson, G. 1983. A method for interpolating scattered data based upon a minimum norm network. *Math. of Computation* 40: 253-271.

Poesen, J. W., J. Nachtergaele, G. Verstraeten, and C. Valentin. 2003. Gully erosion and environmental change: Importance and research needs. *Catena* 50(2): 91-133.

PyWavelets. 2011. Technical API documentation. PyWavelets open source wavelet transform software. Available at: pywavelets.readthedocs.org/en/latest/ref/index.html. Accessed February 2011.

QCoherent. 2011. Getting started with LP360. Madison, Ala.: QCoherent Software. Available at: www.qcoherent.com/products/docs/lp360_gettingstarted.pdf. Accessed February 2011.

Rachman, A., S. H. Anderson, E. E. Alberts, A. L. Thompson, and C. J. Gantzer. 2008. Predicting runoff and sediment yield from a stiff-stemmed grass hedge system for a small watershed. *Trans. ASABE* 51(2): 425-432.

Renard, K. G., G. R. Foster, G. A. Weesies, D. K. McCool, and D. C. Yoder. 1997. *Predicting Soil Erosion by Water: A Guide to Conservation Planning with the Revised Universal Soil Loss Equation (RUSLE)*. Agriculture Handbook No. 703. Washington, D.C.: USDA.

Renka, R. J., and A. K. Cline. 1984. A triangle-based C1 interpolation method. *Rocky Mountain J. Math.* 14(1): 223-237.

Shields, D. F., R. E. Lizotte, and S. S. Knight. 2011. Spatial and temporal water quality variability in aquatic habitats of a cultivated floodplain. *River Res. and Applic.* 29(3): 313-329.

Thorne, C. R., E. H. Grissenger, and J. B. Murphey. 1984. Field study of ephemeral cropland gullies in northern Mississippi. ASAE Paper No. 842550. St. Joseph, Mich.: ASAE.

Thorne, C. R., L. W. Zevenbergen, E. H. Grissinger, and J. B. Murphey. 1986. Ephemeral gullies as sources of sediment. In *Proc. 4th Federal Interagency Sedimentation Conf.*, Vol. 1: 3-152 to 3-161. Reston, Va.: U.S. Geological Survey.

Topcon. 2011. *GLS-1000 Instructional Manual*. Tokyo, Japan: Topcon Corp. Available at: https://positioning.topcon.co.jp/en/document/manual/?dcid=3#sec40. Accessed February 2011.

Valentin, C., J. Poesen, and Y. Li. 2005. Gully erosion: Impacts, factors, and control. *Catena* 63(2-3): 132-153.

Wilson, J. P., and J. C. Gallant. 2000. *Terrain Analysis: Principles and Applications*. New York, N.Y.: John Wiley and Sons.

Zevenbergen, L., and C. Thorne. 1987. Quantitative analysis of land surface topography. *Earth Surf. Proc. Landforms* 12(1): 47-56.

Zhang, W., and D. R. Montgomery. 1994. Digital elevation model grid size, landscape representation, and hydrologic simulations. *Water Resources Res*. 30(4): 1019-1028.

Ziadat, F. M. 2007. Effect of contour intervals and grid cell size on the accuracy of DEMs and slope derivatives. *Trans. in GIS* 11(1): 67-81.